

Article

Improved Representation of Flow and Water Quality in a North-Eastern German Lowland Catchment by Combining Low-Frequency Monitored Data with Hydrological Modelling

Muhammad Waseem ^{*}, Jannik Schilling , Frauke Kachholz and Jens Tränckner 

Faculty of Agriculture and Environmental Sciences, University of Rostock, 18051 Rostock, Germany; jannik.schilling@uni-rostock.de (J.S.); frauke.kachholz@uni-rostock.de (F.K.); jens.traenckner@uni-rostock.de (J.T.)

* Correspondence: muhammad.waseem@uni-rostock.de; Tel.: +49-381-498-3467

Received: 21 May 2020; Accepted: 10 June 2020; Published: 12 June 2020



Abstract: Achievements of good chemical and ecological status of groundwater (GW) and surface water (SW) bodies are currently challenged mainly due to poor identification and quantification of pollution sources. A high spatio-temporal hydrological and water quality monitoring of SW and GW bodies is the basis for a reliable assessment of water quality in a catchment. However, high spatio-temporal hydrological and water quality monitoring is expensive, laborious, and hard to accomplish. This study uses spatio-temporally low resolved monitored water quality and river discharge data in combination with integrated hydrological modelling to estimate the governing pollution pathways and identify potential transformation processes. A key task at the regarded lowland river Augraben is (i) to understand the SW and GW interactions by estimating representative GW zones (GWZ) based on simulated GW flow directions and GW quality monitoring stations, (ii) to quantify GW flows to the Augraben River and its tributaries, and (iii) to simulate SW discharges at ungauged locations. Based on simulated GW flows and SW discharges, NO₃-N, NO₂-N, NH₄-N, and P loads are calculated from each defined SW tributary outlet (SWTO) and respective GWZ by using low-frequency monitored SW and GW quality data. The magnitudes of NO₃-N transformations and plant uptake rates are accessed by estimating a NO₃-N balance at the catchment outlet. Based on sensitivity analysis results, Manning's roughness, saturated hydraulic conductivity, and boundary conditions are mainly used for calibration. The water balance results show that 60–65% of total precipitation is lost via evapotranspiration (ET). A total of 85–95% of SW discharge in Augraben River and its tributaries is fed by GW via base flow. SW NO₃-N loads are mainly dependent on GW flows and GW quality. Estimated SW NO₃-N loads at SWTO_Ivenack and SWTO_Lindenberg show that these tributaries are heavily polluted and contribute mainly to the total SW NO₃-N loads at Augraben River catchment outlet (SWO_Gehmkow). SWTO_Hasseldorf contributes least to the total SW NO₃-N loads. SW quality of Augraben River catchment lies, on average, in the category of heavily polluted river with a maximum NO₃-N load of 650 kg/d in 2017. Estimated GW loads in GWZ_Ivenack have contributed approximately 96% of the total GW loads and require maximum water quality improvement efforts to reduce high NO₃-N levels. By focusing on the impacts of NO₃-N reduction measures and best agricultural practices, further studies can enhance the better agricultural and water quality management in the study area.

Keywords: groundwater and surface water interactions; integrated hydrology; lowlands; MIKE SHE; MIKE 11; water management; water quality

1. Introduction

Lowland catchments are characterized by a high groundwater (GW) table, low flow velocity, flat topography, and a significant presence of organic soils [1–4]. In the past centuries, different anthropogenic activities, such as river regulations, enhanced groundwater abstraction, and provision of artificial drainage to ensure better agricultural activities, have caused an impact on ecology, water balance, and nutrient dynamics, resulting in eutrophication and water quality deterioration [5,6]. Diffuse pollution from agriculture has increased considerably over the past few decades due to human activities related to the surplus use of both organic and synthetic fertilizers [7,8]. Over application of nitrogen (N) fertilizers to the crops in thin soils with steeper terrain causes significant damages to the environmental ecosystem, especially during the wet seasons [9]. Surplus nitrogen input is identified as a key contributor to the increased nutrient concentrations in the surface, ground, and coastal waters [10].

In Europe, agricultural activities continue to affect the surface water (SW) and GW quality in terms of $\text{NO}_3\text{-N}$ pollution [11–13]. The EU nitrate directive was introduced in 1991 to identify and reduce the $\text{NO}_3\text{-N}$ pollution in water bodies (Directive 91/676/EEC), and it focuses on integrated management of water in river catchments to acquire, improve, or maintain a good chemical and ecological status. Despite enormous efforts, a large ratio of European GW and SW bodies still do not comply with the “good chemical and ecological status” according to the defined criteria of the European water framework directive (EU-WFD). One reason is the still-poor identification, quantification, and management of diffuse pollution sources. The EU-WFD demands to reach a good chemical and ecological status of freshwater bodies by the year 2027. In the case of Germany, improvements are required due to the possible surplus use of agricultural fertilizers. Germany is continuously struggling with GW $\text{NO}_3\text{-N}$ concentrations higher than 11.3 mg/L, a threshold for a “good chemical and ecological status” of GW [14,15]. Due to deficiencies in implementing the ordinance of agriculture fertilizer application and surplus use of both synthetic and organic fertilizers, a rise in $\text{NO}_3\text{-N}$ concentrations in comparison to the reported $\text{NO}_3\text{-N}$ concentrations from 2004 to 2007 is observed [16,17]. In 2016, the European court of justice brought legal action against Germany due to deficiencies in implementing the ordinance of agriculture fertilizer applications [7,18].

The whole situation stresses the more effective measures needed to understand and reduce diffuse $\text{NO}_3\text{-N}$ emissions, transport, and transformation processes, especially for lowlands with intensive agricultural activities. This demands high spatio-temporal hydrological and water quality monitoring at a catchment and regional scale. Normally, high-resolution monitoring data in most of the lowland catchments are not available to reliably quantify and access the chemical and ecological status of water bodies and to identify critical areas and/or hidden point sources requiring the maximum measures to reduce the SW and GW $\text{NO}_3\text{-N}$ concentrations. A detailed water and mass balance information is essential to develop and improve the management practices of water resources, as SW and GW interactions mainly control the $\text{NO}_3\text{-N}$ dynamics in lowland rivers [19]. Physically based hydrological models can quantify the GW and SW interactions, and can simulate GW flow directions and SW discharges at ungauged locations. Hydrological modelling results, in combination with low-frequency monitored water quality data, can estimate the SW and GW $\text{NO}_3\text{-N}$ pollution loads at catchment and sub-catchment scales. To select a suitable modelling tool to simulate Augraben catchment (a typical representative of north-eastern Germany lowland catchments), four different process-based models, “SWAT” (soil and water assessment tool), “SWIM” (soil and water integrated model), “HSPF” (hydrological simulation program—FORTRAN), and a coupled “MIKE SHE and MIKE 11” model, are reviewed. These models are compared by concentrating primarily on temperate-climate lowland catchments with intensive agricultural land use. Appendix A shows the summary of reviewed models based on simulated hydrological and hydraulic processes, governing equations, input data requirements, spatial and temporal discretization, and limitations [20–31]. The physically based distributed coupled MIKE SHE and MIKE 11 model is selected in this study to quantify the detailed

water balance, simulation of surface flows at ungauged locations, and interactions of GW and SW at a desired level of complexity.

This study uses available low-frequency monitored flow and water quality data in combination with integrated hydrological and hydraulic modelling to represent the SW and GW hydrology and $\text{NO}_3\text{-N}$ loads in Au Graben River catchment. The research objectives of the present study include: (i) Detailed water balance estimation and quantification of GW and SW interactions, (ii) application of simulated SW discharges at ungauged locations to calculate $\text{NO}_3\text{-N}$ loads at each SW tributary outlet (SWTO), (iii) estimation of the saturated zone represented by each GW quality monitoring station and quantification of GW contribution to the SW $\text{NO}_3\text{-N}$ loads, (iv) identification of critical areas and sources mainly contributing to the water quality deterioration, and (v) estimation of a nutrient balance at Au Graben River catchment outlet to evaluate the magnitude of $\text{NO}_3\text{-N}$ transformations and plant uptakes.

2. Material and Methods

2.1. Study Area

Au Graben River is the largest tributary of the Tollense River in terms of discharge and length. It is located in the lowlands of north-eastern Germany and is representative for the typical lowland flood plains of Central Europe. The Au Graben River has a total length of 18 km up to the gauge station Gehmkow. The area of the Au Graben River catchment up to the gauge station Gehmkow is 90 km². In the study area, the precipitation normally happens throughout the year in Au Graben River catchment, with the most precipitation during the 31 days centred around July. The least precipitation normally occurs around February. On average, the temperature normally varies from -1 to 25 °C, and is rarely below -8 °C or above 31 °C during the course of the year. The wet season lasts from May to February, with more than 24% chance of a given day being a wet day. The drier season lasts from February to May (<https://weatherspark.com/> and <https://dwd.de>). Figure 1a shows the average monthly temperature and precipitation in the study area during 2017. The topography is very flat in the study area. The lowest points at the Au Graben River bed level vary between 40 (u/s) and 28 m (d/s) above NN (Reference Level).

The main tributaries of Au Graben River include Lindenberg, Hasseldorf, and Au II Kentzlin. Three wastewater treatment plants (WWTPs) are located within the Au Graben River catchment: WWTP_Lindenburg, WWTP_Ivenack, and WWTP_Stavenhagen. The treated wastewater is discharged into the Au Graben River and its tributaries, and then finally flows to the Tollense River. Table 1 characterizes the WWTP in terms of populations equivalents (PE) calculated from their inflow loads of chemical oxygen demand (COD), total nitrogen (N), and total phosphorus (P). Additionally, to the domestic wastewater, WWTP_Stavenhagen handles the wastewater from a large potato processing company and shows, therefore, a very high COD load. The nutrient loads are, in comparison, much smaller. The is in the German size class 5, and has fulfilled emission standards of N-inorganic: 13 mg/L and P: 1 mg/L [32]. The rural WWTPs of Lindenberg (activated sludge system) and Ivenack (pond system) are treating less than 1000 PE.

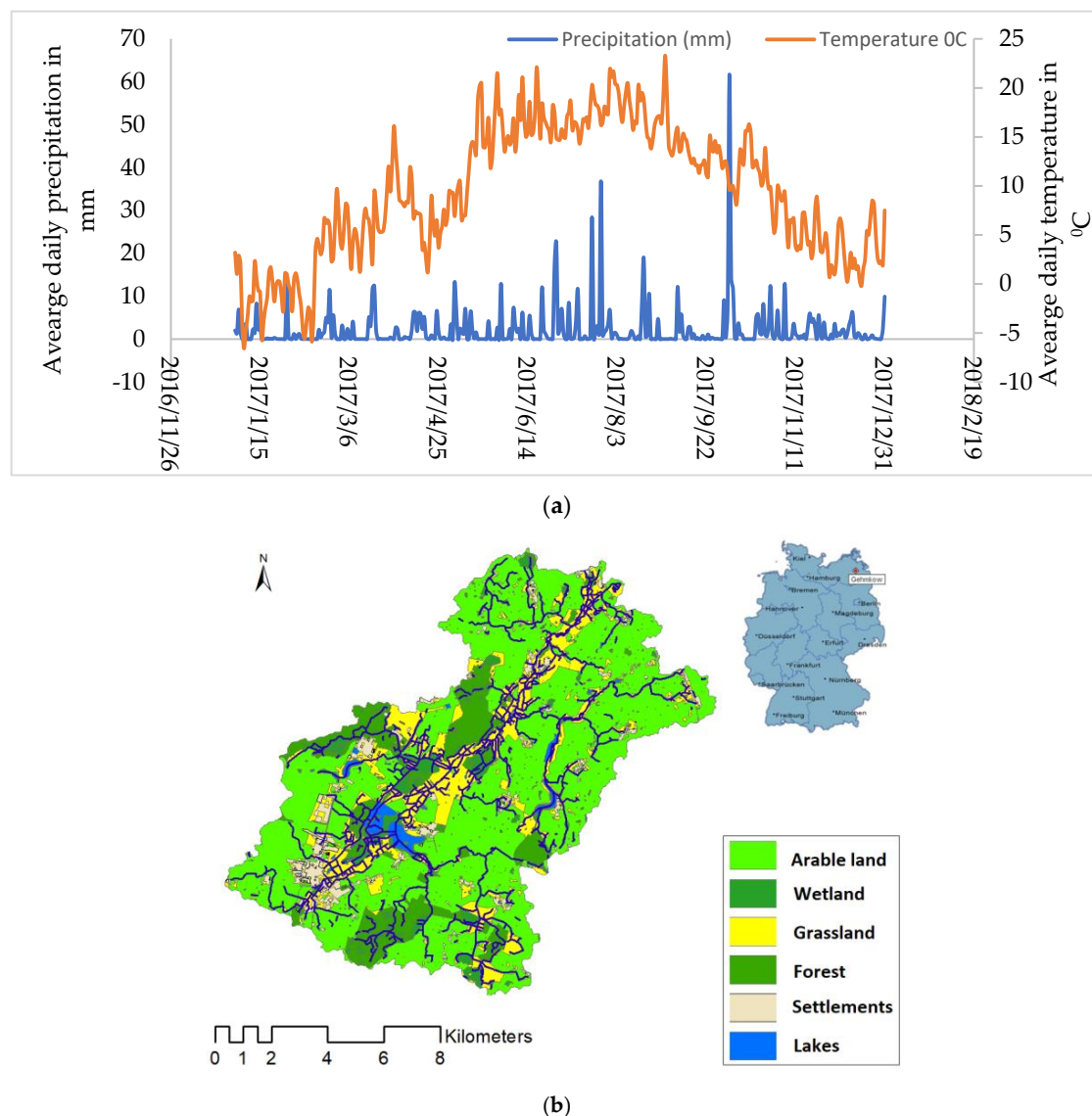


Figure 1. (a) Average daily precipitation and temperature in the study area in 2017. (b) Land use in Augraben River catchment. Land-use, rivers, and lakes data are provided by “Landesamt für Umwelt, Naturschutz und Geologie Mecklenburg Vorpommern (LUNG-MV)” ©.

Table 1. Population equivalent of all three wastewater treatment plants’ (WWTPs’) inflow chemical oxygen demand (COD), total nitrogen (N), and total phosphorus (P).

	Standard Emissions	WWTP Lindenberg		WWTP Ivenack		WWTP Stavenhagen	
	Kg/d-inhabitant	kg/d	PE	kg/d	PE	kg/d	PE
COD	0.12	11.60	96.72	75.90	632.52	12,510.22	104,251.9
N	0.011	1.68674	153.34	4.09	371.86	654.280	59,480
P	0.0018	0.19	107.22	0.9951	552.8	88.304	49,058.18

The Augraben River is still considered heavily loaded with nutrients. In Augraben River catchment, agricultural activities and concentrated animal feeding operations are assumed to be contributing most to the diffuse GW $\text{NO}_3\text{-N}$ pollution. For the implementation of the Nitrates Directive, Germany has formulated a nationwide action programme for the reduction of nitrate applications. Important elements of the Fertilizer Ordinance include the application of permitted amounts of fertilizer during the allowed time periods with a minimum distance to be maintained from the SW bodies. The Revision of the German Fertilizer Ordinance in 2017 specifies only an upper limit for animal manure application, and a farm should, on average, apply less than 170 kg nitrogen per hectare per annum [33].

Due to the increased $\text{NO}_3\text{-N}$ concentrations, the Augraben River catchment is characterized by high primary production of weeds in the vegetation period and the formation of organic sediments. Land use in Augraben River catchment is mainly agricultural. The geology is very heterogeneous and consists mainly of glacial deposits of fluvial sand and glacial till. Due to extreme geological heterogeneity, a large and diverse system of unconfined and confined aquifers with dissimilar flow directions and residence times exists in the lowlands located in north-eastern Germany. The land-use classification in Augraben catchment, shown in Figure 1b, consists of 2% settlements, 2.22% water, 75% arable and grassland, 18% forest area, and 3% miscellaneous. The study area is highly regulated for improved agricultural activities.

2.2. Data Collection

2.2.1. Climate Data

Climate data were collected as accumulated daily rainfall at three climate monitoring stations named Demmin, Gross-Luckow, and Trollenhagen. Demmin is located within the catchment, while Gross-Luckow and Trollenhagen are located nearby but outside the study area. The representative area of each climate station was calculated by the Thiessen Polygon method of interpolation, as shown in Figure 2. The Penman–Monteith method was used to calculate the potential evapotranspiration in the study.

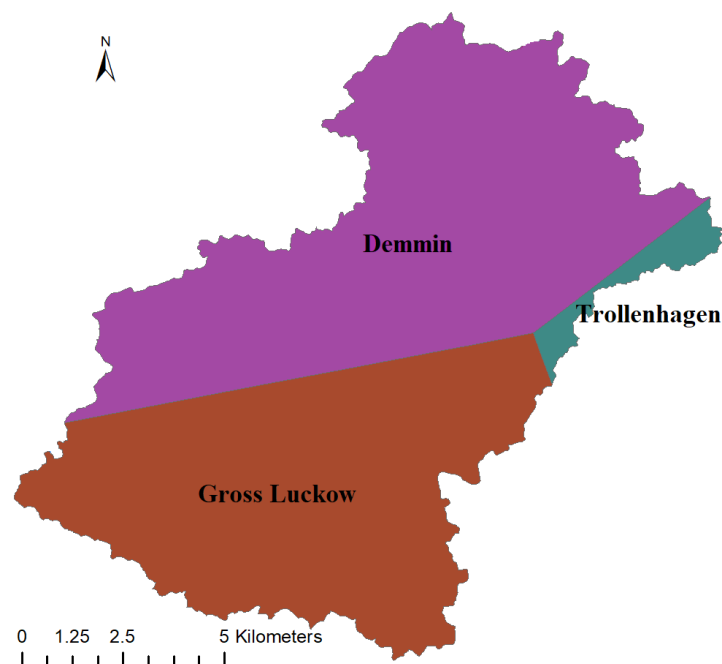


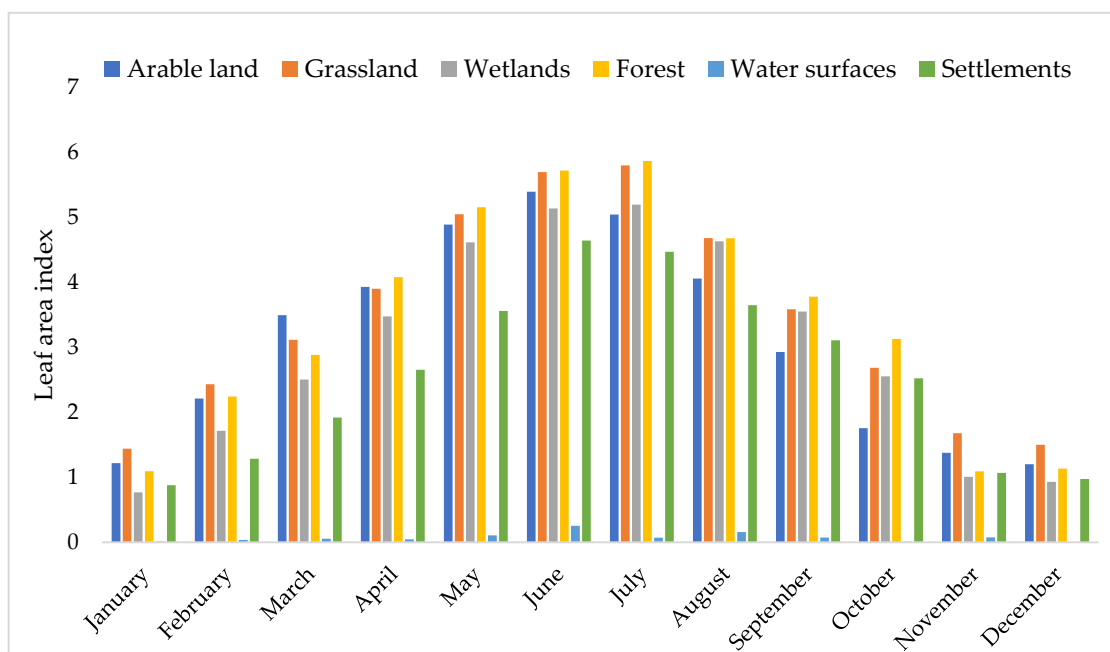
Figure 2. Representative catchment area of each climate monitoring station estimated by the Thiessen Polygon interpolation method.

2.2.2. Land-Use Data

Land use is based on Rapid Eye Archive images (<https://resa.blackbridge.com>). Land-use classification was performed to classify the land use into arable land, forest, grassland, wetland, lakes, and settlement areas. Average root depths (RD) for different land-use classifications during the winter and summer season are shown in Table 2. Leaf area index (LAI) in monthly resolution is presented in Figure 3. RD and LAI were collected from the project KOGGE (www.kogge.auf.uni-rostock.de) conducted in a nearby catchment by University of Rostock.

Table 2. Average root depths (RD) for different land-use classes during winter and summer seasons in Augraben River catchment [34].

Land-Use	Average Root Depth in Winter (mm)	Average Root Depth in Summer (mm)
Arable land	200	600
Wetlands	300	300
Grassland	100	300
Forest	800	800
Settlements	600	600
Water surfaces	0	0

**Figure 3.** Average monthly variation of leaf area index (LAI) in Augraben River catchment [34].

2.2.3. Surface Water Discharge Data

SW flow data at discharge monitoring station Gehmkow were collected from the local environmental protection department (StÄLU-MS) in average daily resolution for a period ranging from 2010 to 2018. Surface flow monitoring station Gehmkow is regarded as Augraben River catchment's outlet and it summarizes all of the upstream monitoring. No surface flow data were available at other independent tributaries (Lindenberg, Hasseldorf, and Ivenack) contributing to the Augraben River. Figure 4 describes the location of the discharge monitoring station and the main tributaries and their outlets in the Augraben River catchment. The collected observed flow data were used later for flow calibration in hydrological modelling.

2.2.4. Water Quality and WWTP Effluent Data

The locations of available GW and SW quality monitoring stations in the Augraben River catchment are shown in Figure 4.

GW quality data were only available for the GW monitoring stations (GWMSs) named GWMS_Törpin and GWMS_Genevzow, and were obtained from StÄLU-MS in yearly resolution. For this study, additional GW samples were collected at three selected GW monitoring stations (GWMS) named GWMS_Lindenberg, GWMS_Hasseldorf, and GWMS_Ivenack at monthly resolution from January 2017 to December 2017. These water samples were analysed for NO₃-N, NO₂-N, and NH₄-N concentrations. To monitor the GW level, five boreholes were installed at GWMS_Genevzow, GWMS_Lindenberg, GWMS_Ivenack, GWMS_Törpin, and GWMS_Hasseldorf. The GW data loggers

provided data with hourly resolution starting from November 2016 to April 2018. Monitored GW levels were used for calibration and validation of the coupled hydrological and hydrodynamic model.

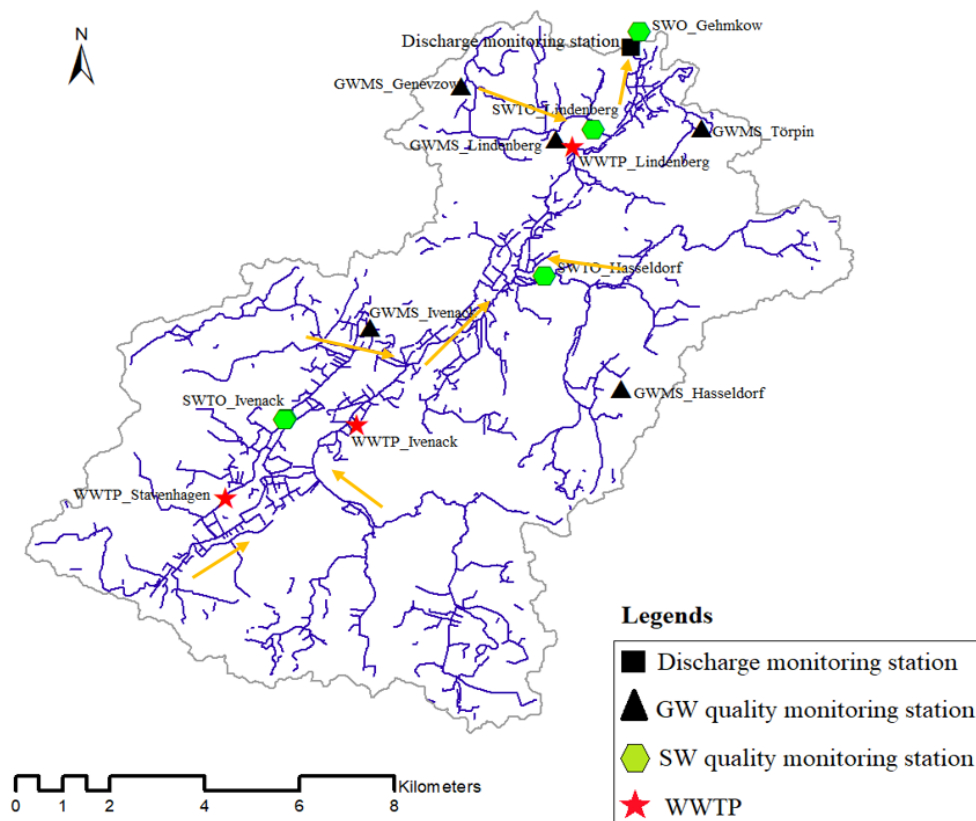


Figure 4. Locations of WWTPs, surface water flow directions (yellow arrows), surface discharge, groundwater quality, and surface water quality monitoring stations in Augrabener River catchment © LUNG-MV.

SW monitoring was performed by StÄLU-MS for $\text{NO}_3\text{-N}$, $\text{NO}_2\text{-N}$, $\text{NH}_4\text{-N}$, and P concentrations at the green marked outflows of sub-catchments. The data are available at monthly resolution, but without the according flow data.

Effluent flow volume and $\text{NO}_3\text{-N}$ and total P concentrations from three WWTPs (WWTP_Ivenack, WWTP_Stavenhagen, and WWTP_Lindenberg) located in the study area were obtained also from StÄLU-MS. SW quality classification was performed by using the German surface water ordinance [35]. The surface water ordinance specifies water quality classes from I (unpolluted) to IV (excessively contaminated).

2.3. MIKE SHE Process-Based Modelling and Mass Balance Framework

As discussed above, MIKE SHE was chosen because of its ability to model GW and SW interactions and dynamics within a catchment in a physical and reliable way [36,37]. The modelling framework describing hydrological processes at the desired level of complexity and spatio-temporal variability used in this study is explained in Figure 5. The digital elevation model (DEM) is used as a data development function to define the catchment boundary and stream network. Spatial disaggregation in MIKE SHE is represented by square grids, and the catchment is distributed into grids of equal size. Each square grid is considered homogeneous. Grid-based formulation of MIKE SHE is compatible with grid-based satellite and weather radar data. The soil column is sectioned into three layers: (i) Surface layer, (ii) soil layer, and (iii) groundwater layer in the MIKE SHE model to simulate GW and SW interactions and flows. The MIKE SHE process-based modelling framework includes spatial lumping

approaches on catchment and sub-catchment levels. Finally, a hydrodynamic model 11 is coupled with the integrated hydrological model MIKE SHE. MIKE 11 can simulate hydraulic structures. The model framework was also chosen to facilitate the later incorporation of transformation processes using Ecolab. Based on the resulting detailed water balance and simulated SW discharges, SW and GW dynamics and SW and GW NO₃-N loads are estimated [38–40].

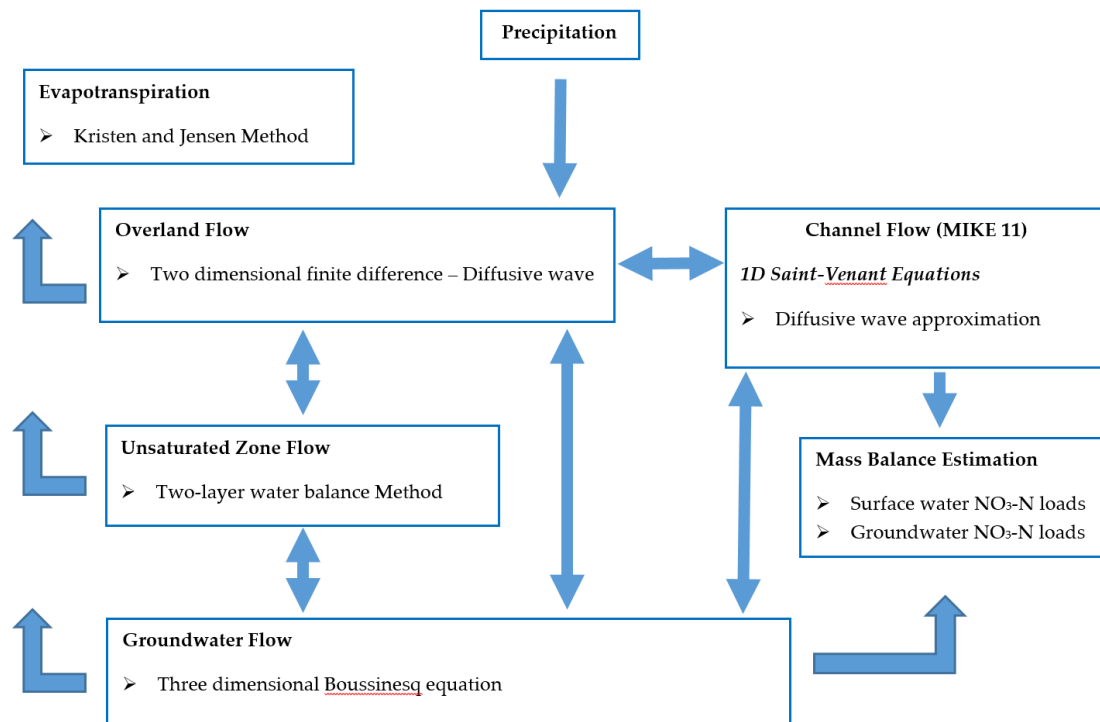


Figure 5. Schematic of the modelling framework used in this study.

The hydrological cycle in MIKE SHE is described by a water movement module (WMM). The WMM of MIKE SHE includes precipitation/interception, evapotranspiration (ET), overland (OL) flow, unsaturated zones (UZ), saturated zones (SZ), and exchange between GW and SW. The ET in MIKE SHE is estimated by using the Kristensen–Jensen method. The flow in UZs is modelled by using a two-layer water balance method. SZ flows in MIKE SHE are simulated by using 3D Boussinesq equation. Simplified diffusive wave approximation of the Saint-Venant equation is used to simulate the river hydrodynamics. The coordinate system “ETRS_1989_UTM_Zone_33N_8stellen”, in metric units, is used in this study. Based on the computational time and resulting model performance, the catchment area is divided into 50 × 50 m grids. The topography in the study area is represented by a digital elevation model (DEM) at 5 m resolution and was provided by StÄLU-MS. Zero-flux and GW inflow and outflow gradients are used as aquifer boundary conditions (BC), as shown in Figure 6a. Catchment boundaries where lateral flows were likely to be negligible based on GW contours are defined as zero-flux BC. However, catchment boundaries where GW lateral inflow and outflow were expected are defined as positive and negative GW gradient BC. The geology is based on borehole log data and is mainly represented by three geological layers in the SZ of Augraben River catchment. The borehole log data from the available 23 boreholes in the study area were used to define the aquifer depth. The river network containing the Augraben River and its tributaries is defined in MIKE 11, as shown in Figure 6b. The coupling of MIKE SHE and MIKE 11 was done dynamically by considering the exchange of data between river links in MIKE 11 to the adjacent MIKE SHE grids after every computational time step [41].

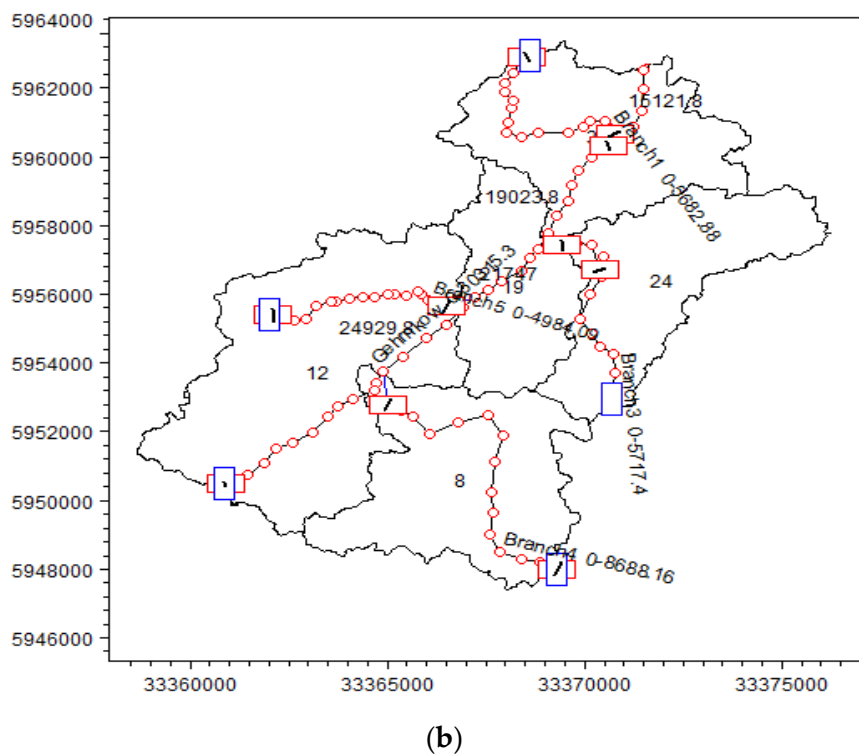
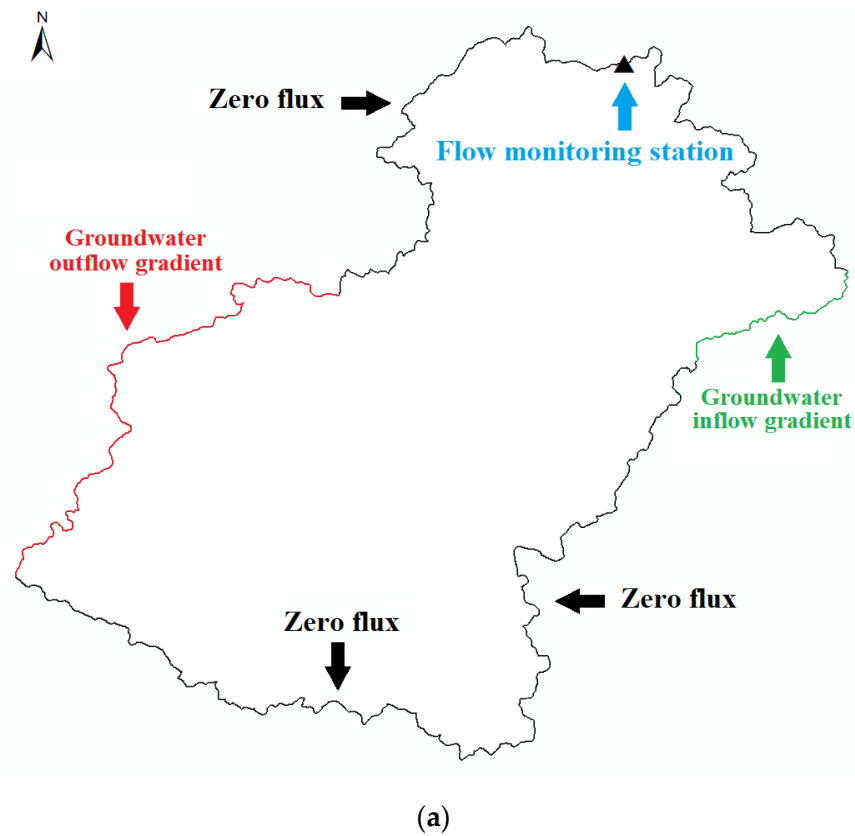


Figure 6. (a) Boundary conditions used in the saturated zone, where the black line is the zero-flux boundary condition, the green line is the inflow groundwater gradient boundary condition, and the red line is the outflow groundwater gradient boundary condition; (b) the Augraben River and its tributaries simulated in this study.

3. Results

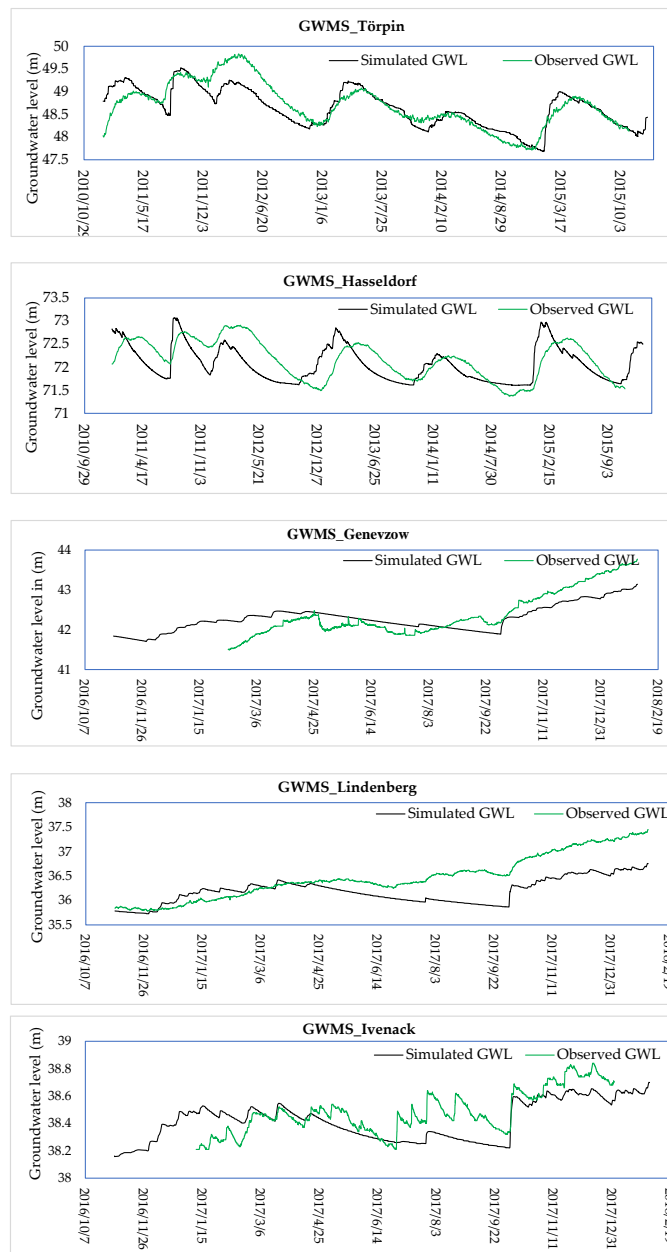
3.1. Coupled Hydrological and Hydraulic Model Calibration and Validation

The most sensitive parameters for the Augrabener River catchment were assessed by sensitivity analysis. Sensitivity analyses were performed by adjusting one parameter value at a time, while keeping others constant in a particular simulation; the magnitude of impact on the simulated results was evaluated for every single parameter value adjustment/change. The resulting most sensitive parameters include initial potential heads, BCs, and saturated hydraulic conductivity. Hourly monitored GW levels (January 2011–December 2015) at GWMS_Törpin, GWMS_Hasseldorf, GWMS_Genevzow, GWMS_Lindenberg, and GWMS_Ivenack were used for the calibration of simulated GW levels by using monitored GW levels (November 2016–April 2018). After calibration, the coupled MIKE SHE and MIKE 11 model was used for generating discharges at ungauged locations. Table 3 describes the calibration parameters, initial and calibration value ranges, selected calibrated values, and statistical performance of GW and SW calibration and validation. Simulated and observed GW levels and SW discharges are shown in Figure 7a,b, respectively. Coupled hydrological and hydraulic model performance was evaluated by using mean absolute error (MAE), root mean square error (RMSE), correlation coefficient (R), and standard deviation residuals (STDres).

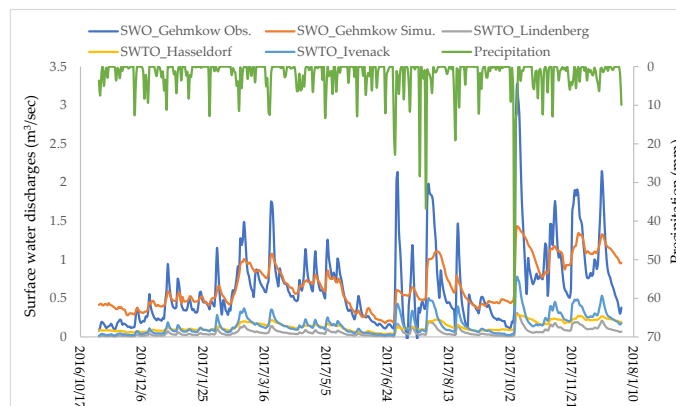
Table 3. Calibration parameters, their ranges, final values, and statistical performance of the coupled model.

Calibration Process				
Selected Parameters	Initial Input Value	Input Range	Calibrated Value	
Hydraulic conductivity [m/s]	A: 1×10^{-6}	1×10^{-10} – 1×10^{10}	1×10^{-4}	
	B: 1×10^{-8}	1×10^{-10} – 1×10^{10}	1×10^{-7}	
	C: 1×10^{-10}	1×10^{-10} – 1×10^{10}	1×10^{-10}	
Specific yield	A: 0.25	1×10^{-10} – 1×10^{10}	0.266	
	B: 0.2	1×10^{-10} – 1×10^{10}	0.20	
	C: 0.1	1×10^{-10} – 1×10^{10}	0.108	
Boundary condition Groundwater inflow and outflow gradients	+ve gradients: 0.0015	0.009–−0.009	0.0036	
	−ve gradients: 0.004	0.009–−0.009	−0.004	
Manning roughness coefficient	Natural channel: 10	10–25	15	
	Weirs or concrete surfaces: 80	80–100	85	
Statistical performance of groundwater calibration				
Monitoring Station	MAE (m)	RMSE (m)	R (Correlation)	STDres
GWMS_Genevzow	1.467	1.508	0.845	0.352
GWMS_Ivenack	1.159	1.166	0.749	0.131
GWMS_Lindenberg	0.478	0.557	0.786	0.351
GWMS_Hasseldorf	1.09	1.107	0.7403	0.24
GWMS_Törpin	1.500	1.555	0.646	0.411
Statistical performance of river flow calibration				
Monitoring Station	MAE (m ³ /s)	RMSE (m ³ /s)	R (Correlation)	STDres
SWO_Gehmkow	0.4514	0.5799	0.7797	0.5299

MAE = “mean absolute error in meters”; RMSE = “root mean square error in meters”; R = “correlation”; STD = “standard deviation residuals”.



(a)



(b)

Figure 7. Observed and simulated groundwater levels (a) and observed and simulated surface water discharges (b) in the study area.

The simulated results show that GW levels are high during the winter and low during the summer season due to respective low and high ET rates. In the current study, the coupled MIKE SHE and MIKE 11 model underestimated the GW levels during high recharge periods. However, model performance was not equally comparable at all monitoring locations, but showed a strong spatio-temporal relationship between simulated GW levels and observed climatic data (precipitation, ET). First, we compare the flow with the only available monitoring station in Gehmkow. Here, the volume balance is met well, while the dynamics are underestimated during high flows and overestimated during low flows with an R^2 (Nash Sutcliffe) of -0.873687 . This possibly happens due to the provision of artificially constructed drainage in MIKE SHE based on the lowest DEM points. The constructed drainage does not fully reflect the installed drainage in the Augrabener River catchment; Figure 1 shows the branched drainage system used in this study. Drainage becomes ineffective when the GW levels fall below the provided artificial drainage levels in MIKE SHE, resulting in smaller GW contribution to the Augrabener River and its tributaries. Afterwards, the calibrated model was applied to calculate flows at the ungauged locations.

3.2. Water Balance Estimation

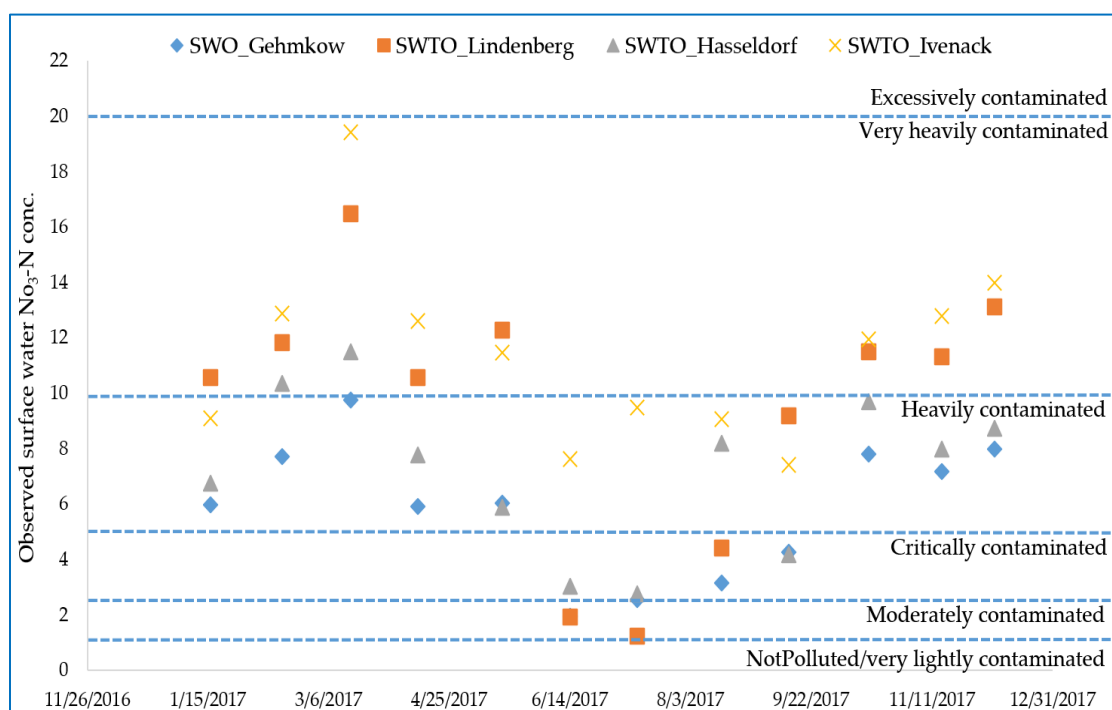
A detailed yearly water balance was performed for the Augrabener River catchment for 2010–2018. Each hydrological year was considered from 1 October to 30 September of the upcoming year based on local conditions. In this study, the hydrological model gets its total water input via precipitation and SZ GW inflow. The total water budget was further divided into ET, surface runoff, change in UZ and SZ storage, and GW and SW interactions. Water balance error was estimated based on total inflows (precipitation, surface and subsurface GW inflow), outflows (ET, overland flow, surface and subsurface GW outflow, GW and SW interactions), and change in UZ and SZ storage. The water balance error of 2% during the calibration period shows the suitable model performance during the simulation period of 2010–2018. Detailed water balance results show that ET loss represents an approximate average of 60–65% of the total precipitation in the study area. The GW contribution to the Augrabener River and its tributaries as a base flow and the SW contribution to the GW as infiltration and percolation show the exchange of flows between MIKE SHE and MIKE 11. SW discharge is mainly fed by GW. The GW contribution to total SW discharges accounts for up to 85–95%. The water balance results show a small decrease in SZ storage over the period of the last eight hydrological years. Table 4 shows the detailed water balance for the Augrabener River catchment; all values are in millimetres (mm). Positive and negative storage change represents the ascending and descending change in water stored in SZ and UZ.

Table 4. Water balance for the Augrabener catchment (90 km²) during hydrological years 2010–2018; all values are in millimetres (mm).

Water Balance Components (mm)	2010–2011	2011–2012	2012–2013	2013–2014	2014–2015	2015–2016	2016–2017	2017–2018	2010–2018
Precipitation	804	511	597	573	599	502	767	447	4814
Evapotranspiration	473	376	445	456	401	367	482	316	3324
Canopy storage change	0	0	0	0	0	0	0	0	0
Overland flow to the river	59	38	37	26	35	34	37	44	311
Snow storage change	0	0	0	0	0	0	0	0	0
Overland storage change	8	−2	−4	2	1	0	6	−7	5
UZ storage change	−24	20	−6	6	1	−26	29	−44	−42
SZ storage change	22	−146	−80	−95	−21	−50	39	−53	−388
SZ drain to river	123	90	79	62	68	66	68	79	638
Infiltration	373	138	182	124	213	180	264	204	1681
Exfiltration	88	61	58	42	54	53	52	68	477
UZ boundary inflow	0	0	0	0	0	0	0	0	0
UZ boundary outflow	3	1	1	1	1	1	2	2	13
SZ boundary inflow	61	55	50	43	43	42	38	43	377
SZ boundary outflow	202	187	175	159	155	152	143	152	1330

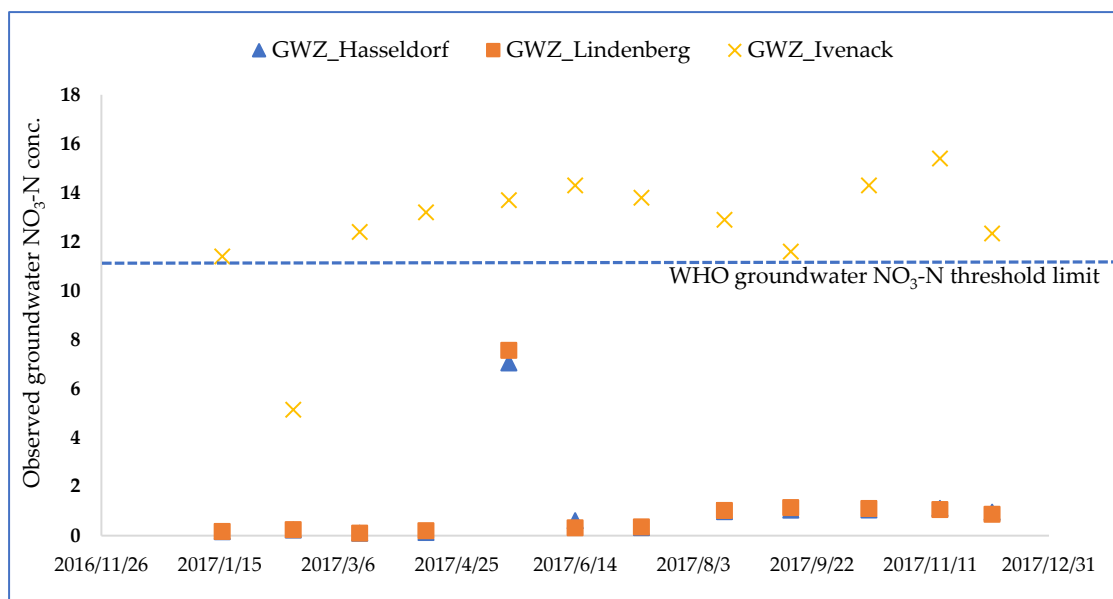
3.3. Surface Water and Ground Water Quality

Observed SW and GW quality data in Augraben River catchment were partially measured (at officially existing monitoring locations) and partially obtained from the local environmental protection department in Augraben River catchment. Observed SW and GW $\text{NO}_3\text{-N}$ concentrations were distributed into pollution classes according to the federal surface water ordinance [35] and the World Health Organization's (WHO) [15] guidelines for $\text{NO}_3\text{-N}$ in GW, respectively. In terms of SW quality, 35.41% of the collected SW samples showed $\text{NO}_3\text{-N}$ concentrations belonging to the category of very heavily contaminated rivers. A total of 43.75% of the SW samples fell under the category of heavily contaminated and 6.25% moderately contaminated. None of the SW samples showed concentrations belonging to the category of lightly or non-polluted rivers. Observed $\text{NO}_3\text{-N}$ concentrations and their respective pollution categories are shown in Figure 8. Classification at the tributary scale shows that measured $\text{NO}_3\text{-N}$ concentrations at the tributary outlets named SWTO_Lindenberg and SWTO_Ivenack come under the water quality class of very heavily polluted, as the measured $\text{NO}_3\text{-N}$ concentrations are clearly elevated, and concentration is reduced only in months from June to September, but still lies in the category of heavily polluted rivers. For approximately similar land-use conditions in the study area, low SW $\text{NO}_3\text{-N}$ concentrations were observed at SWTO_Hasseldorf. This shows that the SWTO_Lindenberg and SWTO_Ivenack water quality monitoring stations were possibly influenced by the point sources contributing to SW pollution. The observed SW $\text{NH}_4\text{-N}$ concentrations also lie in the category of very highly contaminated rivers. In terms of GW $\text{NO}_3\text{-N}$ concentrations, 30% of the GW samples collected in the study area in 2017 showed higher concentrations than the threshold limit defined by the WHO for GW. GW quality classification shows that the GW zone (GWZ) Ivenack $\text{NO}_3\text{-N}$ concentrations throughout the year are higher than the threshold value of 11.3 mg/L defined by the WHO. However, GWZ_Lindenberg and GWZ_Hasseldorf show lower $\text{NO}_3\text{-N}$ concentrations.



(a)

Figure 8. Cont.



(b)

Figure 8. Classification of the Augraben River's and its tributaries' surface water (a) and groundwater quality (b) based on the federal surface water ordinance [35].

ET follows the intensity of incoming solar radiation and the resulting number of sunshine hours during the course of the year. Low ET in combination with moderate precipitation during the winter and spring seasons results in higher discharges. Fertilizer is applied primarily in spring and (to a lower extent) in early autumn, and plant nitrogen uptake follows the pattern of ET in the study area. Total monthly $\text{NO}_3\text{-N}$ loads at SWO_Gehmkow follow the seasonal pattern of the total monthly runoff volume. GW quality monitoring is influenced by various factors. Observed $\text{NO}_3\text{-N}$ concentrations at a particular GWMS do not wholly represent the water quality status of a GWZ. The reliability of GW monitoring is influenced by the selection and location of the boreholes [42,43]. In the study area, qualitative monitoring was performed at two hydrological boreholes bi-yearly and at three boreholes monthly. MIKE SHE coupled with a hydrodynamic model MIKE 11 simulated the GW levels and flow directions in the study area. In order to quantify the representative area of the saturated zone under each monitored borehole, the calibrated GW model MIKE SHE coupled with a hydrodynamic model MIKE 11 was applied to estimate GW flow directions. The constructed GW contours explain that the GW flow direction is towards the Augraben River and its tributaries throughout the catchment, and that underlines that GW largely contributes to the surface discharges. However, GWZ_Ivenack is special, as GW contributes to the tributary and also passes underneath the river towards lower GW elevations. The GW table, in general, follows the topography of the catchment; however, in some areas, it differs from the topography. Water in the saturated zone flows due to differences in the energy state of the water, described by the term hydraulic head. The GW flow is determined by the gradient in the hydraulic head and the hydraulic conductivity, which is an empirical constant describing the ability of geological media to transmit water. Based on GW flow directions and available GW monitoring stations in the study area, the representative area was estimated according to each available GW quality monitoring station. The Augraben River catchment is divided into three GWZs (GWZ_Lindenberg, GWZ_Hasseldorf, and GWZ_Ivenack), as shown in Figure 9. The boreholes named GWMS_Genezow and GWMS_Lindenberg are located in GWZ_Lindenberg, boreholes GWMS_Törpin and GWMS_Hasseldorf are located in GWZ_Hasseldorf, and GWMS_Ivenack is located in the GWZ_Ivenack. GW flow paths vary greatly in length and depth depending on where the GW recharges and the travel time within a catchment. In highly polluted areas, it is necessary

to conduct reliable monitoring of GW, as better GW quality assessment will help in counteracting the negative effects of pollution [44–47].

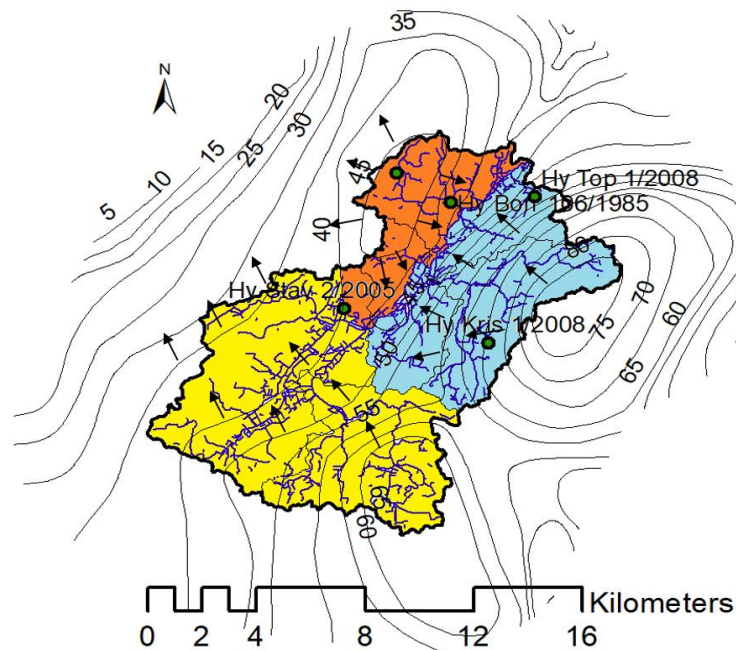
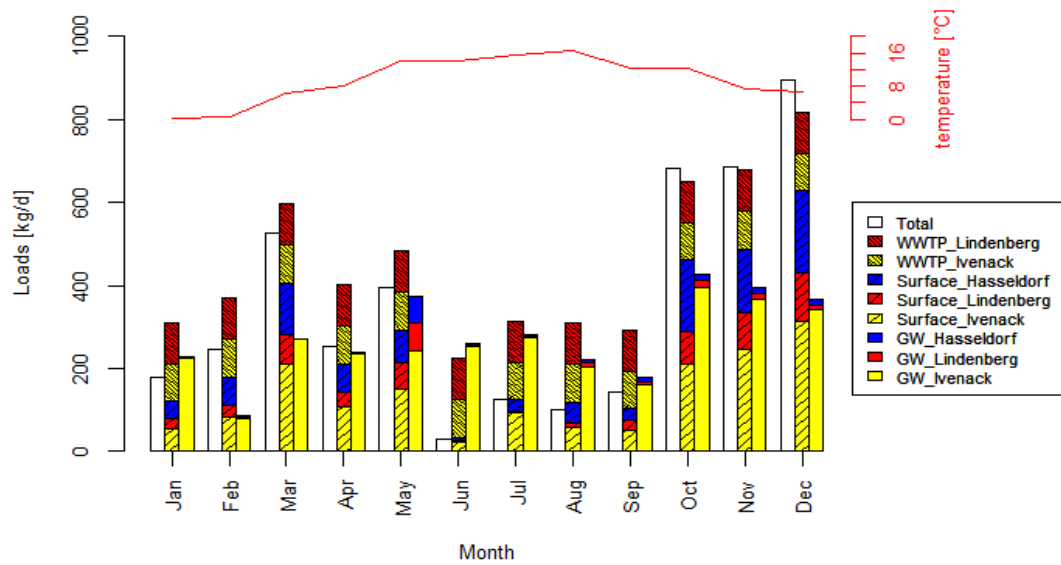


Figure 9. Based on simulated groundwater contours and flow directions, the defined sub-catchments are possibly represented by each available groundwater quality monitoring station; GWZ_Lindenberg (red), GWZ_Hasseldorf (blue), and GWZ_Ivenack (yellow).

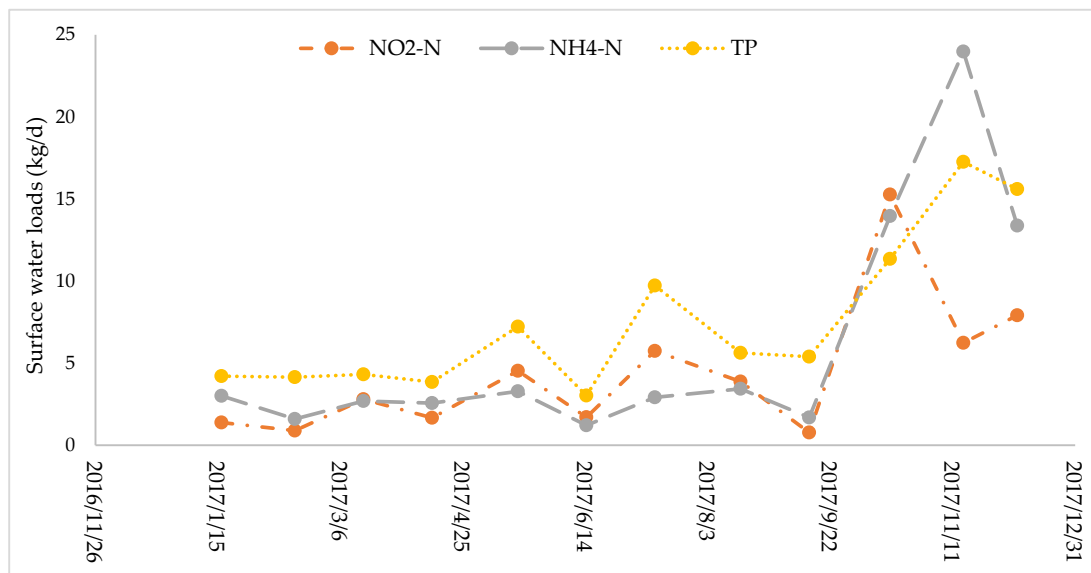
3.4. Nutrient Balance at Catchment Outlet

The uncertainties in average concentration and load estimations can be reduced by increasing the sampling frequency. However, the SW and GW sampling, sample transport, and laboratory procedures are expensive and laborious. A favourable approach is the load estimation from available observed low-frequency concentration data. The explanatory strength of commonly available continuous measurements, such as precipitation, discharge, and GW levels at limited locations, in combination with hydrological modelling can access water quality variation at ungauged locations. Most of the commonly available hydrological measurements (precipitation, temperature, wind speed, etc.) are relatively inexpensive and often available near SW and GW quality monitoring locations to facilitate the quantitative management of water. First, simulated SW discharges obtained from the coupled MIKE SHE and MIKE 11 model were used to estimate the SW $\text{NO}_3\text{-N}$, $\text{NO}_2\text{-N}$, $\text{NH}_4\text{-N}$, and total P loads at SWTO_Lindenberg, SWTO_Hasseldorf, SWTO_Ivenack, and SWO_Gehmkow. WWTPs and their effluent $\text{NO}_3\text{-N}$ and total P loads were added to estimate the $\text{NO}_3\text{-N}$ balance and $\text{NO}_3\text{-N}$ transformations at the Augraben River outlet. Secondly, simulated GW flows for each respective GWZ were used to calculate the GW $\text{NO}_3\text{-N}$ loads in all three GWZs, named as GWZ_Lindenberg (red), GWZ_Hasseldorf (blue), and GWZ_Ivenack (yellow). It is estimated that GWZ_Lindenberg and GWZ_Hasseldorf contribute the least to the GW $\text{NO}_3\text{-N}$ loads, while GWZ_Ivenack, based on measured concentrations and GW volumes, contributes a maximum of up to 96% in terms of GW $\text{NO}_3\text{-N}$ loads. The possible causes behind the higher observed GW $\text{NO}_3\text{-N}$ concentrations at GWZ_Ivenack in comparison to GW $\text{NO}_3\text{-N}$ concentrations at GWZ_Lindenberg and GWZ_Hasseldorf include (1) infiltration from two nearby WWTPs, where WWTP_Stavenhagen is a large-scale WWTP, and effluent $\text{NO}_3\text{-N}$ load discharged into the tributary Ivenack can infiltrate into the GW. As $\text{NO}_3\text{-N}$ loads are detectable at SWTO_Ivenack, that is why WWTP $\text{NO}_3\text{-N}$ loads are not specified separately in Figure 10a. Total effluent $\text{NO}_3\text{-N}$ loads from WWTP_Stavenhagen account for 47.84 kg/d. Direct GW infiltration is negligible or zero, as WWTP_Stavenhagen does not allow GW

infiltration due to its construction and operational design. WWTP_Ivenack is a pond-type WWTP and can possibly influence the GW quality due to infiltration. However, its small-scale operational capacity also limits its possible contribution to GW quality. Stormwater runoff from biogas plants and other agricultural facilities was identified in other studies as a potentially relevant pollution source [48]. As the land use type is nearly the same in the Augraben River catchment, higher GW concentration could also point to a different fertilizer usage behaviour in different areas of the catchment. A high spatio-temporal monitoring is necessary to evaluate the GW and SW quality variation at a smaller scale, but it is evident from the estimated GW loads that the highest GW loads occur in June, July, August, and September.



(a)



(b)

Figure 10. (a) Surface water tributary outlet (SWTO), WWTP, and groundwater zone (GWZ) $\text{NO}_3\text{-N}$ loads in the Augraben River catchment and their relation with water temperature; (b) calculated $\text{NO}_2\text{-N}$, $\text{NH}_4\text{-N}$, and total P loads at the Augraben River outlet.

The nutrient balance of the estimated SW loads at the Augraben River outlet is shown in Figure 10a. It reveals that, especially in summer, the total $\text{NO}_3\text{-N}$ loads at SWO_Gehmkow are lower than the sum of the calculated SWTO_Lindenberg, SWTO_Hasseldorf, SWTO_Ivenack, and WWTP effluent loads. Here, an inverse relationship between $\text{NO}_3\text{-N}$ loads and observed water temperature is visible. The higher reduction in SW $\text{NO}_3\text{-N}$ loads at the outlet during the summer months indicates significant transformation either by denitrification or by increased plant growth. In winter or during times with low water temperatures, the biological processes are reduced to a very low level while base flow increases, resulting in higher nitrate loads. The difference between total SW loads at SWO_Gehmkow and the summed loads from SWTO_Lindenberg, SWTO_Hasseldorf, SWTO_Ivenack, and WWTP gives the magnitude of the transformation and plant uptake, on average, of up to 50% of total loads at SWO_Gehmkow during the months of June, July, August, and September. The loads of $\text{NO}_2\text{-N}$, $\text{NH}_4\text{-N}$, and total P are shown in Figure 10b. In general, SWO_Gehmkow's water quality status lies in the strongly polluted river category.

The main findings of nutrient balance at SWO_Gehmkow include (1) estimation of SW and GW loads from each SWTO and representative GWZ; (2) estimation of $\text{NO}_3\text{-N}$ transformation and plant uptake rate; (3) critical SW and GWZ identifications requiring maximum measures to reduce $\text{NO}_3\text{-N}$ loads; (4) explanation of possible $\text{NO}_3\text{-N}$ hotspots influencing the water quality. It is recommended that the locations of water quality monitoring stations should be reconsidered based on tributaries with heavy pollution and GW flow directions to accurately point out the hotspots. This study highlights the need for further necessary measures to achieve the EU-WFD goals and demands a stronger process-oriented monitoring. A valuable improvement would already be flow measurement in parallel with grab sampling.

4. Discussion

The bi-directional coupled hydrologic (MIKE SHE) and hydraulic (MIKE 11) model was applied to the Augraben River catchment, a tributary of the Tollense River. The Augraben River catchment represents common features of the European lowland catchments, such as shallow GW tables, GW and SW interactions, control structures, provision of artificial drainage, periodic inundation, etc. Due to these features, the modelling approach explained in the current study has a huge potential to simulate/predict the lowland response to anthropogenic activities and expected changing climatic conditions and to provide guidelines for better conservation and management practices of susceptible catchments.

4.1. Method Strengths

Water Balance: Water balance estimation in a river catchment predicts the detailed surface water and groundwater interactions. A detailed water balance explains the main water loss components and will help in developing watershed management practices and better informed policy decisions [49,50]. In this study, the calibrated coupled MIKE SHE and MIKE 11 model has predicted the water balance with an error of less than 2%. ET is a main water loss component. Surface discharges are mainly fed by groundwater, and groundwater flow is a dominant pathway in the Augraben River catchment. Higher groundwater contributions to surface water discharges in lowland Augraben River catchment are following the hydrological studies conducted in lowland catchments in north-eastern Germany [1,51–53]. Overland flow or direct runoff is very low in comparison to other water balance components. Lowland catchments are characterized with low direct runoff flows in contrast to mountainous catchments, where direct surface water runoff is a dominant pathway [54,55]. The resulting groundwater contribution to surface groundwater and surface water interactions mainly controls the pollutant ($\text{NO}_3\text{-N}$) dynamics and influences the surface water and groundwater quality [56,57].

Simulated Surface Flow at Ungauged Locations and Groundwater Levels: The lack of surface water discharge monitoring stations in small or remote catchments is a hurdle in defining the catchment management measures [58,59]. In the Augraben River catchment located in north-eastern Germany,

discharge data were only available at the catchment outlet. No measured discharges were available at the Augrabener River's tributaries. In the current study, the groundwater levels and surface discharges were successfully generated by the integrated coupled hydrological and hydraulic model (MIKE SHE and MIKE 11). The simulated discharge at Gehmkow shows good agreement between simulated and observed discharge with an R (correlation) of 0.7797 and RMSE of 0.579. The performance of the calibrated model is not the same at all locations due to the defined simplifications during the modelling procedure.

Mass Balance and NO₃-N Transformation Rates: The NO₃-N pollution of SW and GW is a major environmental problem, especially in lowlands with intensive agriculture and related farm activities. Achievement of environmental sustainability requires the detailed assessment of spatial and temporal variation of water quality at the catchment and regional scale. River mass balance methods using observed or simulated flows and pollutant concentrations can be helpful in describing the magnitude and extent of existing pollutant loads along a river [60,61]. Based on coupled hydrological and hydraulic model results, we have successfully estimated the NO₃-N loads at the catchment and sub-catchment scale by combining low-frequency monitoring data with hydrological modelling. GW levels were available at only two monitoring stations. In terms of water quality assessment and its variations at a catchment scale, limited monitoring data were available. This enhances both the explanatory strength of generally available and inexpensive quantitative hydrological data and the (so far, only) qualitative status information from grab sampling [62]. The responses of NO₃-N and P concentrations can be plausibly linked to the hydrological dynamics of SW and GW, triggered by the meteorological input. Combining these data with measured emission data of WWTP, a trustworthy source apportionment between diffuse and known point sources is feasible. In summertime, the measured load is lower than the predicted sum. The difference can be a rough estimate of NO₃-N transformations and plant uptake rates. The results of this study demonstrate, in line with similar studies [63,64], that using the explanatory strength of quantitative hydrological data can significantly improve load estimates.

4.2. Method Weakness

Short-term dynamics of SW quality variations are not captured by common low-frequency grab sampling. The low-frequency monitoring provides an overview of the average concentrations of chemical species and suggests some general processes that may explain the observed data. The added value of high-frequency monitoring is the possibility of capturing diurnal cycles and transient events that help relate the causes and effects of human activities and storms. High-frequency monitoring can go much further in the interpretation of the data and can more precisely uncover and/or confirm rapid processes at work in the system [65–67]. The method can reliably estimate the contribution of diffuse sources. To explain loads from point sources, additional data are needed. Here, only the data of WWTP emissions could be included. Polluted storm water runoff could be an additional nutrient input, which was not addressed so far.

From the qualitative perspective, the method is purely data-driven. It could be considered to expand the hydrological model by additional transformation processes. This was out of the scope of this study, aiming at an improved interpretation of available monitoring data. However, with regard to designing mitigation measures, an expanded process model would be worthwhile.

4.3. Transfer of Methodology to Other Lowland Catchments

The method of the applied coupled hydrological model in combination with low-frequency monitored data can be transferred at the desired rate of complexity to similar lowland catchments. According to our assessment, the chosen model setup was best suited to simulate the typical characteristics of lowland catchments, such as (i) artificial drainage to support better agriculture activities, (ii) backwater effect due to smaller slopes, (iii) complex SW and GW interactions, and (iv) river flows. The subsequent mass balance and source apportionment are valuable to prioritize and allocate measures to reduce nutrient emissions.

However, the method is not delimited to the model framework chosen here. Under different boundary conditions, other models could be equally or even more advisable. Four different process-based models—“soil and water assessment tool” (SWAT), “soil and water integrated model” (SWIM), “hydrological simulation program—FORTRAN” (HSPF), and a coupled “MIKE SHE and MIKE 11” model—were compared in this study. The DHI’s combined tools and SWAT were more suitable for simulating the desired hydrological processes, but in the case of river hydraulics, the integrated coupling between MIKE SHE and MIKE 11 is a plus. In the case of SWAT, it needs to be coupled with another tool to model the hydraulics in the Augrabener River, as SWAT does not simulate the backwater effects and operation of control structures (weirs, gates, etc.). However, both the SWAT and DHI tools are more data-demanding in comparison to SWIM and HSPF. HSPF, in turn, already contains tools to model nitrogen transformation and transport processes along the hydrological system, which is helpful for designing mitigation measures. Most of the input data and governing equations in the case of SWIM and SWAT are similar. SWIM does not simulate water bodies (ponds and lakes), wetlands, and drainage systems.

4.4. Usefulness of Model Predictions and Future Applications

The analysis of the model’s predictions/future forecasts and deficiencies related to model structure and availability of data offers better understanding of the processes (water and nutrient) at different temporal (monthly and annual) and spatial scales (catchment, sub-catchment, river). In the Augrabener River catchment, critical areas were identified where in-depth additional investigations are required. In particular, the specific emissions in the Ivenack sub-catchment were noticeably higher than in the other sub-catchments. Accordingly, monitoring and systems analysis should be strengthened here to support better catchment management practices/activities. As expected, higher $\text{NO}_3\text{-N}$ loads occur outside the vegetation period during autumn and winter. Estimated $\text{NO}_3\text{-N}$ loads are heavily influenced by temperature. The differences between forecasted and measured nitrate loads in SW can be interpreted/transformed/removed; loads are very low during the winter and autumn seasons due to the lower temperatures. Environmental conditions during the summer and spring seasons favour higher plant uptake and increased microbial activities.

4.5. Key Parameters to Reduce Nitrogen Inputs

The study was performed in the phase when the new fertilizer regulation came into effect. The observed state still represents the conditions before the stronger regulations. It can be assumed that the reduced tolerated nitrogen surplus will, in the longer term, be viable in reduced nitrogen concentrations at the GW, and will accordingly reduce loads to the SW. The increased specific loads from the Ivenack catchment may not only be due to farming activities. For several years, polluted stormwater runoff from sealed areas on animal farms and biogas plants has been suspected to be an important nutrient point source. In addition, the view should be open to so far unidentified polluters. Regular water quality monitoring and sampling frequency at a higher resolution will help in reliable and precise assessment of the status of surface and groundwater bodies.

5. Conclusions

The $\text{NO}_3\text{-N}$ pollution of SW and GW is a major environmental problem, especially in lowlands with intensive agriculture and related farm activities. Achievement of environmental sustainability requires the detailed assessment of spatial and temporal variation of water quality at the catchment and regional scale. The required high-resolution spatial and temporal monitoring for profound assessment is often in contrast to the existing data. This study, conducted in a north-eastern German lowland catchment, aims at improving the expressiveness of inconsistent monitoring data by combining it with a coupled hydrologic model. The main conclusions are:

- By combining a coupled SW/GW model with spatially and temporally scarce grab samples, the dominant nutrient entry pathways can be roughly allocated and quantified.
- Process-based hydrological modelling can help in defining SW and GW quality monitoring locations and schedules.
- The modelling approach can be transferred to similar lowlands, and a calibrated coupled model can be used to identify the priority areas to reduce nutrient pollution. Differences between accumulated loads and measured total loads can be used as rough estimates for instream transformation processes.

The SW quality in the investigated Augraben River system varies—applying national and international assessment schemes—between moderately to very heavily polluted. Total load reached a maximum NO₃-N load of 650 kg/d in 2017. In the summer season, GW loads' contribution is higher in comparison to the total load at the catchment outlet. However, in winter, a higher SW load is calculated with a small increase in GW load. NO₃-N loads from point sources, such as WWTP, cannot be neglected. In this study, estimated GW loads in GWZ_Ivenack contributed the most to the total GW loads. WWTP_Stavenhagen, on average, contributes 25% of the total NO₃-N load at SWTO_Ivenack. Areas with higher NO₃-N loads (GWZ_Ivenack in this study) require maximum water quality improvement efforts to reduce high NO₃-N levels.

Author Contributions: M.W. and J.T. contributed most to the manuscript in terms of model setup, simulation, calibration, original manuscript writing, and review. J.T. and M.W. conceived and designed the overall study concept and are responsible for the consultations regarding model simulation results, comparisons, manuscript writing, proofreading, and manuscript modification. J.S. and F.K. were involved in model setup, data analysis, and manuscript modifications. All authors have read and agreed to the published version of the manuscript.

Funding: This study was performed within an HEC/DAAD PhD grant in collaboration with the research project Bootmonitoring in the BMBF program (FKZ: 033W039B). The APC was funded by the Open Access Department, University of Rostock.

Acknowledgments: We would like to thank the “State Agency for Environment, Nature Conservation, and Geology (LUNG-MV)” and “State Office for Agriculture and Environment (StÄLU-MS) Mecklenburg-Vorpommern, Germany” for their kindness in providing the essential data in order to conduct this study. DHI was very helpful during the study period and provided the MIKE SHE and MIKE 11 student license free of cost to the author. The authors are thankful to the Open Access Department, University of Rostock, for their willingness to pay the article processing charges.

Conflicts of Interest: The authors declare no conflict of interest.

Appendix A

Review summary of the selected modelling tools based on their ability to simulate the lowland catchments.

	Hydrological Processes			
	SWAT	SWIM	HSPF	MIKE SHE
Interception		-	Interception	Interception
Evapotranspiration (ET)		Evapotranspiration	Evapotranspiration	Evapotranspiration
Infiltration (I)		Infiltration	Infiltration	Infiltration
Percolation		Percolation	Percolation	Percolation
Subsurface flow		Subsurface flow	Subsurface flow	Subsurface flow
Baseflow		Baseflow	Baseflow	Baseflow
Surface runoff		Surface runoff	Surface runoff	Surface runoff
Drainage		-	-	Drainage
Pump flow		-	-	Pump flow
Urban drainage		-	-	Urban drainage

SWAT	SWIM	HSPF	MIKE SHE and MIKE 11
-	-	-	River Pumps
-	-	-	Backwater effect
-	-	-	Control structures
-	-	-	Operational strategies
Governing Equations			
SWAT			
Runoff volume	Modified Soil Conservation Service (SCS) Curve Number or Green and Ampt infiltration equation		
Peak runoff rate	Rational formula or the SCS TR-55 method		
Subsurface flow and percolation	Kinematic storage routine equation; is based on several input data regarding hillslope, field capacity, the volume of soil water, soil porosity, and hydraulic conductivity		
Potential evapotranspiration	<ul style="list-style-type: none"> • Hargreaves equation • Priestley–Taylor equation • Penman–Monteith equation 		
Flow rate and velocity	<ul style="list-style-type: none"> • Manning’s equatio 		
Sediment yield	Modified Universal Soil Loss Equation		
Flow routing	“Muskingum routing method” or “variable storage routing method”		
SWIM			
Surface runoff	The non-linear function of precipitation and a retention coefficient		
Subsurface flow	Kinematic storage routine equation		
Potential evapotranspiration	Priestley–Taylor or Penman–Monteith		
Sediment yield	Modified Universal Soil Loss Equation		
HSPF			
Infiltration	Empirical method based on the type of soil and available storage		
Flow rate and velocity	Manning’s equation		
Flow routing	Kinematic wave routing or storage routing		
MIKESHE			
Surface runoff	1D diffusive wave Saint Venant equation		
Unsaturated zone flow	<ul style="list-style-type: none"> • Richards equation • Gravity flow • Two-layer water balance method 		
Saturated zone flow	<ul style="list-style-type: none"> • 3D finite difference method • Linear reservoir method 		
Overland flow	2D finite difference diffusive wave equation		
Evapotranspiration	Kristensen and Jensen method Two-Layer UZ/ET module		
Flow routing	<ul style="list-style-type: none"> • No routing • Muskingum method • Muskingum–Cunge method 		
Difficulties or Limitations			
SWAT	<ul style="list-style-type: none"> • SWAT does not simulate sub-daily events; e.g., a single storm event or flood routing of a single event. • SWAT does not model the denitrification process during water quality modelling. • SWAT does simulate organic P and inorganic P, but takes into account the adsorption or desorption of inorganic P to particles. 		

SWIM	<ul style="list-style-type: none"> • SWIM does not simulate the water quality of reservoirs, ponds, and lakes • Simulation accuracy is not only directly related to the grid size of the spatial input data, but it is also determined by optimal model parameters 			
HSPF	<ul style="list-style-type: none"> • SWIM simulates many physical processes based on empirical relations. • Metrological factors affect the model results' accuracy • Limited to 1D flows and well-mixed rivers • Insensitive to spatial variations 			
MIKE SHE	<ul style="list-style-type: none"> • Extensive input data requirements 			
Input data				
SWAT				
Climate	Hydrogeology	Soil data	Land use	Topography
Daily precipitation	Groundwater table height	Soil thickness or depth	Land use/land cover	Digital elevation model (DEM)
Air temperature (max and min)	Aquifer storage	Bulk density	Leaf area index (LAI)	-
Solar radiation	Drainage	Soil moisture content	Plant root depth (RD)	-
Wind speed	Irrigation	Soil hydraulic conductivity	-	-
Evapotranspiration	Saturated hydraulic conductivity	Porosity	-	-
Humidity	Groundwater recharge	Soil texture	-	-
-	Aquifer specific yield	-	-	-
-	Groundwater abstraction rates	-	-	-
SWIM				
Climate	Hydrogeology	Soil data	Land use	Topography
Precipitation	Groundwater table height	Soil thickness or depth	Land use/land cover	Digital elevation model (DEM)
Air temperature (max, min, and average)	Aquifer storage	Bulk density	Leaf area index (LAI)	-
Solar radiation	Drainage	Soil moisture content	Plant root depth (RD)	-
Evapotranspiration	Saturated hydraulic conductivity	Soil hydraulic conductivity	-	-
-	Groundwater recharge	Porosity	-	-
-	Aquifer specific yield	Field capacity	-	-
-	-	Wilting point	-	-
HSPF				
Climate	Hydrogeology	Soil data	Land use	Topography
Precipitation	surface water storage	Soil thickness or depth	Land use/land cover	Digital elevation model (DEM) or sub-basin area and average slope
Air temperature	Aquifer storage	Bulk density	-	
Dew point temperature	PH	Soil moisture content	-	
Solar radiation	Subsurface flow storage	Soil hydraulic conductivity	-	
Wind speed	-	Infiltration capacity	-	
Evapotranspiration	-	Soil texture	-	
Humidity	-	-	-	
Vapor pressure	-	-	-	

MIKE SHE				
Climate	Hydrogeology	Soil data	Land use	Topography
Precipitation	Groundwater table	Geological layers	Land use/land cover	Digital elevation model (DEM)
Air temperature	Aquifer storage	Bulk density	Vegetation type	-
Solar radiation	Specific yield	Soil moisture content	Vegetation height	-
Wind speed	Saturated hydraulic conductivity	Soil hydraulic conductivity	Leaf area index	-
Evapotranspiration	Groundwater extraction	Porosity	Root depth	-
Humidity	Groundwater recharge rate	Soil texture	-	-
Vapor pressure	Drainage	-	-	-
Daily sunshine hours	Irrigation	-	-	-
-	Depth of the saturated zone	-	-	-
-	Capillary storage	-	-	-
Spatial and temporal discretization				
SWAT	SWIM	HSPF	MIKE SHE	
Spatial: Flexible, Temporal: Continuous	Spatial: Flexible, Temporal: Daily	Spatial: Flexible, Temporal: Flexible or user-defined time step	Spatial: Flexible, Temporal: Event-based and continuous	
Basic Purpose				
SWAT	SWAT's principle purpose is to compute runoff and loadings from rural areas and watersheds with intensive agriculture. SWAT evaluates the effects of different management practices and decisions on water resources, as well as agricultural pollutants in large river catchments.			
SWIM	The SWIM model was established to examine the impacts of climate and land-use changes at the regional level.			
HSPF	The HSPF model was developed to simulate both catchment hydrology and water quality.			
MIKE SHE	The key purpose of the MIKE SHE model is the integrated modelling of evapotranspiration, groundwater, surface water, and groundwater recharge.			

References

- Lam, Q.D.; Schmalz, B.; Fohrer, N. Assessing the spatial and temporal variations of water quality in lowland areas, Northern Germany. *J. Hydrol.* **2012**, *438*, 137–147. [[CrossRef](#)]
- Schmalz, B.; Springer, P.; Fohrer, N. Variability of water quality in a riparian wetland with interacting shallow groundwater and surface water. *J. Plant. Nutr. Soil Sci.* **2009**, *172*, 757–768. [[CrossRef](#)]
- Krause, S.; Bronstert, A.; Zehe, E. Groundwater–surface water interactions in a North German lowland floodplain—implications for the river discharge dynamics and riparian water balance. *J. Hydrol.* **2007**, *347*, 404–417. [[CrossRef](#)]
- Hesse, C.; Krysanova, V.; Pätzold, J.; Hattermann, F.F. Eco-hydrological modelling in a highly regulated lowland catchment to find measures for improving water quality. *Ecol. Model.* **2008**, *218*, 135–148. [[CrossRef](#)]
- Sophocleous, M. Interactions between groundwater and surface water: The state of the science. *Hydrogeol. J.* **2002**, *10*, 52–67. [[CrossRef](#)]
- Kieckbusch, J.J.; Joachim, S. Nitrogen and phosphorus dynamics of a re-wetted shallow-flooded peatland. *Sci. Total Environ.* **2007**, *380*, 3–12. [[CrossRef](#)]
- Kirschke, S.; Häger, A.; Kirschke, D.; Völker, J. Agricultural Nitrogen Pollution of Freshwater in Germany. The Governance of Sustaining a Complex Problem. *Water* **2019**, *11*, 2450. [[CrossRef](#)]
- de Wit, M.; Behrendt, H.; Bendoricchio, G.; Bleuten, W.; van Gaans, P. The contribution of agriculture to nutrient pollution in three European rivers, with reference to the European Nitrates Directive. *Eur. Water Manag. Online* **2002**, 1–19.

9. Zhang, W.; Li, H.; Kendall, A.D.; Hyndman, D.W.; Diao, Y.; Geng, J.; Pang, J. Nitrogen transport and retention in a headwater catchment with dense distributions of lowland ponds. *Sci. Total Environ.* **2019**, *683*, 37–48. [[CrossRef](#)] [[PubMed](#)]
10. Heathwaite, L.; Sharpley, A.; Gburek, W. A conceptual approach for integrating phosphorus and nitrogen management at watershed scales. *J. Environ. Qual.* **2000**, *29*, 158–166. [[CrossRef](#)]
11. Hildebrandt, A.; Guillamón, M.; Lacorte, S.; Tauler, R.; Barceló, D. Impact of pesticides used in agriculture and vineyards to surface and groundwater quality (North Spain). *Water Res.* **2008**, *42*, 3315–3326. [[CrossRef](#)]
12. Schoumans, O.F.; Chardon, W.J.; Bechmann, M.E.; Gascuel-Oudou, C.; Hofman, G.; Kronvang, B.; Dorioz, J.M. Mitigation options to reduce phosphorus losses from the agricultural sector and improve surface water quality: A review. *Sci. Total Environ.* **2014**, *468*, 1255–1266. [[CrossRef](#)] [[PubMed](#)]
13. Böhlke, J.K. Groundwater recharge and agricultural contamination. *Hydrogeol. J.* **2002**, *10*, 153–179. [[CrossRef](#)]
14. He, B.; Kanae, S.; Oki, T.; Hirabayashi, Y.; Yamashiki, Y.; Takara, K. Assessment of global nitrogen pollution in rivers using an integrated biogeochemical modeling framework. *Water Res.* **2011**, *45*, 2573–2586. [[CrossRef](#)] [[PubMed](#)]
15. Xue, Y.; Song, J.; Zhang, Y.; Kong, F.; Wen, M.; Zhang, G. Nitrate pollution and preliminary source identification of surface water in a semi-arid river basin, using isotopic and hydrochemical approaches. *Water* **2016**, *8*, 328. [[CrossRef](#)]
16. Commission Staff Working Document Executive Summary of the Impact Assessment Accompanying the Document Proposal for a Regulation of the European Parliament and of the Council Laying down Rules on the Making Available on the Market of CE Marked Fertilising Products and Amending Regulations (EC) No 1069/2009 and (EC) No 1107/2009. Available online: <https://eur-lex.europa.eu/legal-content/EN/TXT/?uri=CELEX%3A52016SC0065> (accessed on 20 May 2020).
17. Directive, N. *Nitrate Pollution in the Groundwater Resources of the Public Drinking Water Supply*; Water Solutions: Stuttgart, Germany, 2017; pp. 25–35.
18. Härtel, J. *Das EuGH-Urteil vom 21. Juni 2018 zum Verstoß Gegen die EU-Nitratrichtlinie Durch die Bundesrepublik Deutschland: Seine Relevanz für die Richtlinienkonformität des Neuen Düngerechts*; Rechtsgutachten Erstellt im Auftrag des Verbands Kommunaler Unternehmen e.V.: Europa-Universität Viadrina Frankfurt, 2018. Available online: https://www.vku.de/fileadmin/user_upload/Verbandsseite/Themen/Umwelt/21_10_2018_Prof_Dr_Ines_Haertel_Gutachten_EuGH_Urteil_Nitratrichtlinie.pdf (accessed on 10 May 2020).
19. Winter, T.C. Relation of streams, lakes, and wetlands to groundwater flow systems. *Hydrogeol. J.* **1999**, *7*, 28–45. [[CrossRef](#)]
20. Jiang, S.; Michael, R. Hydrological Water Quality Modelling of Nested Meso Scale Catchments. Ph.D. Thesis, Technische Universität Braunschweig, Braunschweig, Germany, 2014.
21. Dhami, B.S.; Pandey, A. Comparative review of recently developed hydrologic models. *J. Indian Water Resour. Soc.* **2013**, *33*, 34–41.
22. Gao, L.; Li, D. A review of hydrological/water-quality models. *Front. Agric. Sci. Eng.* **2014**, *1*, 267–276. [[CrossRef](#)]
23. Benaman, J.; Shoemaker, C.A.; Haith, D.A. Calibration and validation of soil and water assessment tool on an agricultural watershed in upstate New York. *J. Hydrol. Eng.* **2005**, *10*, 363–374. [[CrossRef](#)]
24. Shoemaker, L.; Dai, T.; Koenig, J.; Hantush, M. *TMDL Model Evaluation and Research Needs*; National Risk Management Research Laboratory: US Environmental Protection Agency: Cincinnati, OH, USA, 2005.
25. Fehér, J.; Muerth, M. *Water Models and Scenarios Inventory for the Danube Region*; Report EUR 27357EN; European Commission Joint Research Centre Institute for Environment and Sustainability: Luxembourg, 2015; Available online: <https://core.ac.uk/download/pdf/38630655.pdf> (accessed on 10 April 2020).
26. Ward, G.H.; Jennifer, B. *A Survey and Review of Modeling for TMDL Application in Texas Watercourses*; Center for Research in Water Resources, University of Texas: Austin, TX, USA, 1999.
27. Kauffeldt, A.; Wetterhall, F.; Pappenberger, F.; Salamon, P.; Thielen, J. Technical review of large-scale hydrological models for implementation in operational flood forecasting schemes on continental level. *Environ. Model. Softw.* **2016**, *75*, 68–76. [[CrossRef](#)]
28. Chen, Y.; Li, W.; Fang, G.; Li, Z. Hydrological modeling in glacierized catchments of central Asia—status and challenges. *Hydrol. Earth Syst. Sci.* **2017**, *21*. [[CrossRef](#)]
29. Krysanova, V.; Fred, H.; Rank, W. Development of the ecohydrological model SWIM for regional impact studies and vulnerability assessment. *Hydrol. Process. Int. J.* **2005**, *19*, 763–783. [[CrossRef](#)]

30. Waseem, M.; Kachholz, F.; Klehr, W.; Tränckner, J. Suitability of a Coupled Hydrologic and Hydraulic Model to Simulate Surface Water and Groundwater Hydrology in a Typical North-Eastern Germany Lowland Catchment. *Appl. Sci.* **2020**, *10*, 1281. [[CrossRef](#)]
31. Waseem, M.; Frauke, K.; Jens, T. Suitability of common models to estimate hydrology and diffuse water pollution in North-eastern German lowland catchments with intensive agricultural land use. *Front. Agric. Sci. Eng.* **2018**, *5*, 420–431. [[CrossRef](#)]
32. Jardin, N. Vereinheitlichung und Herleitung von Bemessungswerten für Abwasseranlagen (A 198). In Proceedings of the Regen-und Mischwasserbehandlung Seminar, Würzburg, Technische Akademie Hannover, Germany, 23–24 September 2003.
33. Kuhn, T. *The Revision of the German Fertiliser Ordinance in 2017*; No. 1548-2017-3861; Institute for Food and Resource Economics, University Bonn: Bonn, Germany, 2017.
34. Tränckner, H. *KOGGE Kommunale Gewässer Gemeinschaftlich Entwickeln—Ein Handlungskonzept für Kleine Urbane GEWÄSSER am Beispiel der Hanse- und Universitätsstadt Rostock*; Universität Rostock: Rostock, Germany, 2018.
35. Verordnung zum Schutz der Oberflächengewässer (Oberflächengewässerverordnung; OGewV) vom 20. Juni 2016. In: BGBl., 2016, I, S. 1 373). Available online: https://www.gesetze-im-internet.de/ogewv_2016/OGewV.pdf (accessed on 3 May 2020).
36. Thompson, J.R. Modelling the impacts of climate change on upland catchments in southwest Scotland using MIKE SHE and the UKCP09 probabilistic projections. *Hydrol. Res.* **2012**, *43*, 507–530. [[CrossRef](#)]
37. Singh, C.R.; Thompson, J.R.; French, J.R.; Kingston, D.G.; Mackay, A.W. Modelling the impact of prescribed global warming on runoff from headwater catchments of the Irrawaddy River and their implications for the water level regime of Loktak Lake, northeast India. *Hydrol. Earth Syst. Sci.* **2010**, *14*, 1745–1765. [[CrossRef](#)]
38. Butts, M.B.; Overgaard, J.; Graham, D.; Dubicki, A.; Strońska, K.; Szalinkska, W.; Larsen, O. Process-based Hydrological Modelling Framework MIKE SHE for Flood Forecasting on the Upper and Middle Odra. In Proceedings of the ICID 21st European Regional Conference, Frankfurt (Oder), Germany; Slubice, Poland, 15–19 May 2005.
39. Thai, T.H.; Tri, D.Q. Combination of hydrologic and hydraulic modeling on flood and inundation warning: Case study at Tra Khuc-Ve River basin in Vietnam. *Vietnam J. Earth Sci.* **2019**, *41*, 240–251. [[CrossRef](#)]
40. Altaf, Y.; Manzoor, A.; Mohammad, F. Modelling snowmelt runoff in Lidder River Basin using coupled model. *Int. J. River Basin Manag.* **2020**, *18*, 167–175. [[CrossRef](#)]
41. Ivanescu, V.; Radu, D. Deriving Rain Threshold for Early Warning Based on a Coupled Hydrological-Hydraulic Model. *Math. Model. Civ. Eng.* **2016**, *12*, 10–21. [[CrossRef](#)]
42. Hosseini, M.; Reza, K. A data fusion-based methodology for optimal redesign of groundwater monitoring networks. *J. Hydrol.* **2017**, *552*, 267–282. [[CrossRef](#)]
43. Gomo, M.; Vermeulen, D.; Lourens, P. Groundwater sampling: Flow-through bailer passive method versus conventional purge method. *Nat. Resour. Res.* **2018**, *27*, 51–65. [[CrossRef](#)]
44. Grath, J.; Scheidleder, A.; Uhlig, S.; Weber, K.; Kralik, M.; Keimel, T.; Gruber, D. *The EU Water Framework Directive: Statistical Aspects of the Identification of Groundwater Pollution Trends, and Aggregation of Monitoring Results*; Austrian Federal Ministry of Agriculture and Forestry, Environment and Water Management: Vienna, Austria, 2001; Final Report.
45. Jousma, G.; Roelofsen, F.J. *World-Wide Inventory on Groundwater Monitoring*; Report nr. GP1; International Groundwater Resources Assessment Center: Delft, The Netherlands, 2004.
46. Nielsen, D.M.; Gillian, N. *The Essential Handbook of Ground-Water Sampling*; CRC Press, Taylor and Francis Group: Boca Raton, FL, USA, 2006.
47. Quevauviller, P.; Fouillac, A.M.; Grath, J.; Ward, R. *Groundwater Monitoring; Water Quality Measurements Series*; Willey: New York, NY, USA, 2009; p. 428.
48. Cramer, M.; Rinas, M.; Kotzbauer, U.; Tränckner, J. Surface contamination of impervious areas on biogas plants and conclusions for an improved stormwater management. *J. Clean. Prod.* **2019**, *217*, 1–11. [[CrossRef](#)]
49. Yapiyev, V.; Skrzypek, G.; Verhoef, A.; Macdonald, D.; Sagintayev, Z. Between boreal Siberia and arid Central Asia—Stable isotope hydrology and water budget of Burabay National Nature Park ecotone (Northern Kazakhstan). *J. Hydrol. Reg. Stud.* **2020**, *27*, 100644. [[CrossRef](#)]
50. Yapiyev, V.; Skrzypek, G.; Verhoef, A.; Macdonald, D.; Sagintayev, Z. A proportionality-based multi-scale catchment water balance model and its global verification. *J. Hydrol.* **2020**, *582*, 124446.

51. Smith, A.; Tetzlaff, D.; Gelbrecht, J.; Kleine, L.; Soulsby, C. Riparian wetland rehabilitation and beaver re-colonization impacts on hydrological processes and water quality in a lowland agricultural catchment. *Sci. Total Environ.* **2020**, *699*, 134302. [[CrossRef](#)] [[PubMed](#)]
52. Waseem, M.; Tatyana, K.; Jens, T. Groundwater Contribution to Surface Water Contamination in a North German Low Land Catchment with Intensive Agricultural Land Use. *J. Water Resour. Prot.* **2018**, *10*, 231. [[CrossRef](#)]
53. Lam, Q.D.; Britta, S.; Nicola, F. The impact of agricultural Best Management Practices on water quality in a North German lowland catchment. *Environ. Monit. Assess.* **2011**, *183*, 351–379. [[CrossRef](#)] [[PubMed](#)]
54. Van Griensven, A.; Meixner, T.; Grundwald, S.; Bishop, T.; Diluzio, A.; Srinivasan, R. A global sensitivity analysis tool for the parameters of multi-variable catchment models. *J. Hydrol.* **2006**, *324*, 10–23. [[CrossRef](#)]
55. Lenhart, T.; Eckhardt, K.; Fohrer, N.; Frede, H.-G. Comparison of Two Different Approaches of Sensitivity Analysis. *Phys. Chem. Earth Parts A/B/C* **2002**, *27*, 645–654. [[CrossRef](#)]
56. Dahm, C.N.; Grimm, N.B.; Marmonier, P.; Valett, H.M.; Vervier, P. Nutrient dynamics at the interface between surface waters and groundwaters. *Freshw. Biol.* **1998**, *40*, 427–451. [[CrossRef](#)]
57. van Geer, F.C.; Kronvang, B.; Broers, H.P. High-resolution monitoring of nutrients in groundwater and surface waters: Process understanding, quantification of loads and concentrations, and management applications. *Hydrol. Earth Syst. Sci.* **2016**, *20*, 3619. [[CrossRef](#)]
58. Jia, P.; Liu, R.; Ma, M.; Liu, Q.; Wang, Y.; Zhai, X.; Wang, D. Flash Flood Simulation for Ungauged Catchments Based on the Distributed Hydrological Model. *Water* **2019**, *11*, 76. [[CrossRef](#)]
59. Chouaib, W.; Alila, Y.; Caldwell, P.V. On the use of mean monthly runoff to predict the flow–duration curve in ungauged catchments. *Hydrol. Sci. J.* **2019**, *64*, 1573–1587. [[CrossRef](#)]
60. Gates, T.K.; Cox, J.T.; Morse, K.H. Uncertainty in mass-balance estimates of regional irrigation-induced return flows and pollutant loads to a river. *J. Hydrol. Reg. Stud.* **2018**, *19*, 193–210. [[CrossRef](#)]
61. Vogt, R.J.; Sharma, S.; Leavitt, P.R. Direct and interactive effects of climate, meteorology, river hydrology, and lake characteristics on water quality in productive lakes of the Canadian Prairies. *Can. J. Fish. Aquat. Sci.* **2018**, *75*, 47–59. [[CrossRef](#)]
62. Rico, A.; Arenas-Sánchez, A.; Alonso-Alonso, C.; López-Heras, I.; Nozal, L.; Rivas-Tabares, D.; Vighi, M. Identification of contaminants of concern in the upper Tagus river basin (central Spain). Part 1: Screening, quantitative analysis and comparison of sampling methods. *Sci. Total Environ.* **2019**, *666*, 1058–1070. [[CrossRef](#)]
63. Ivanovsky, A.; Criquet, J.; Dumoulin, D.; Alary, C.; Prygiel, J.; Duponchel, L.; Billon, G. Water quality assessment of a small peri-urban river using low and high frequency monitoring. *Environ. Sci. Process. Impacts* **2016**, *18*, 624–637. [[CrossRef](#)]
64. Jomaa, S.; Aboud, I.; Dupas, R.; Yang, X.; Rozemeijer, J.; Rode, M. Improving nitrate load estimates in an agricultural catchment using Event Response Reconstruction. *Environ. Monit. Assess.* **2018**, *190*, 330. [[CrossRef](#)] [[PubMed](#)]
65. Jones, C.S.; Wang, B.; Schilling, K.E.; Chan, K.S. Nitrate transport and supply limitations quantified using high-frequency stream monitoring and turning point analysis. *J. Hydrol.* **2017**, *549*, 581–591. [[CrossRef](#)]
66. van der Grift, B.; Broers, H.P.; Berendrecht, W.; Rozemeijer, J.; Osté, L.; Griffioen, J. High-frequency monitoring reveals nutrient sources and transport processes in an agriculture-dominated lowland water system. *Hydrol. Earth Syst. Sci.* **2016**, *20*, 1851–1868. [[CrossRef](#)]
67. Drake, C.W.; Jones, C.S.; Schilling, K.E.; Amado, A.A.; Weber, L.J. Estimating nitrate-nitrogen retention in a large constructed wetland using high-frequency, continuous monitoring and hydrologic modeling. *Ecol. Eng.* **2018**, *117*, 69–83. [[CrossRef](#)]

